

Dynamics of ion–molecule reactions from beam experiments: A historical survey



Zdenek Herman^{a,*}, Jean H. Futrell^b

^aJ. Heyrovský Institute of Physical Chemistry, v.v.i., Academy of Sciences of the Czech Republic, Dolejškova 3, 18223 Prague 8, Czech Republic

^bPhysical Sciences Division, Pacific Northwest National Laboratory, P.O. Box 999, Richland, WA 99352, USA

ARTICLE INFO

Article history:

Received 7 April 2014

Received in revised form 9 June 2014

Accepted 10 June 2014

Available online 12 June 2014

Keywords:

Ion–molecule reactions

Dynamics

Beam scattering

ABSTRACT

A historical survey of beam scattering studies of ion–molecule reactions from the sixties up to the present time is presented. The centers of research that developed key instrumentation for these studies and early achievements in characterizing basic collisional mechanisms in scattering experiments are reviewed. Important classes of cation–molecule reaction dynamics, impulsive atom-transfer, reaction complexes, electron transfer (charge transfer) dynamics and the dynamics of negative ion–molecule reactions are described. Selected specific examples of ion–molecule reaction dynamics, including multiply-charged and ion–surface collisions, are briefly presented.

© 2014 Elsevier B.V. All rights reserved.

1. Introduction

Ion–molecule reactions were historically studied under single-collision conditions in ion sources of mass spectrometers and a large amount of data on reaction sequences and cross sections had been generated by the mid-sixties. An exciting new development in reaction kinetics—namely, beam scattering experiments and studies of neutral–neutral chemical reactions under single collision conditions—was introduced in the same time frame. Pioneering experiments of Datz and Taylor [1] initiated a new era of investigating the dynamics of chemical reactions of neutrals [2] and was the inspiration for extending analogous beam techniques to the investigation of chemical reactions of ions.

By physically separating ion formation and reaction chambers, beam techniques introduced significantly improved control of the translational energy of ion reactants. Mass, direction, and energy (and possibly internal state) of the ion reactant was fully defined prior to reaction. Tandem methods [3], guided-beam methods [4] and merged-beam methods [5] made it possible to determine total (integral) cross sections of ion–molecule processes and their dependence on collision energy. These powerful tools are reviewed elsewhere in this Special Issue and will not be described here; rather, we focus on techniques that specifically include scattering measurements of reactants and products and make it possible to obtain scattering diagrams and differential cross section of reaction products. A modification of the guided-beam method

using guided field variation as a way to obtain differential cross sections has also been described [6].

Beam scattering studies determine not only the identity of reaction products, but also their velocity and angular distribution, and often provide information on their internal state. The distinctive characteristic that ion reactions are readily investigated at collision energies from quasi-thermal up to many electron volts enabled a deeper general insight into the influence of translational energy on chemical processes. The sensitivity of mass spectrometric detection also enables detailed studies of low abundance products. More specifically, ion–neutral crossed beam experiments provide us with the following details of their reaction dynamics:

- Total and differential cross sections as a function of well-defined collision energy.
- Cross sections as a function of internal state of the ion reagents.
- Velocities and internal states of the products.
- Angular distribution of the products.

We also note that several reviews of beam scattering studies have been published that should be consulted for additional information [7–13].

2. The transition to molecular beam techniques

Fig. 1 illustrates schematically the components of an apparatus that enables this class of measurements. The required features are an appropriate ion source for preparation of a state-selected ion beam, its mass analysis and velocity selection, state and velocity selection of the neutral beam, and mass and velocity analysis of the

* Corresponding author.

E-mail address: zdenek.herman@jh-inst.cas.cz (Z. Herman).

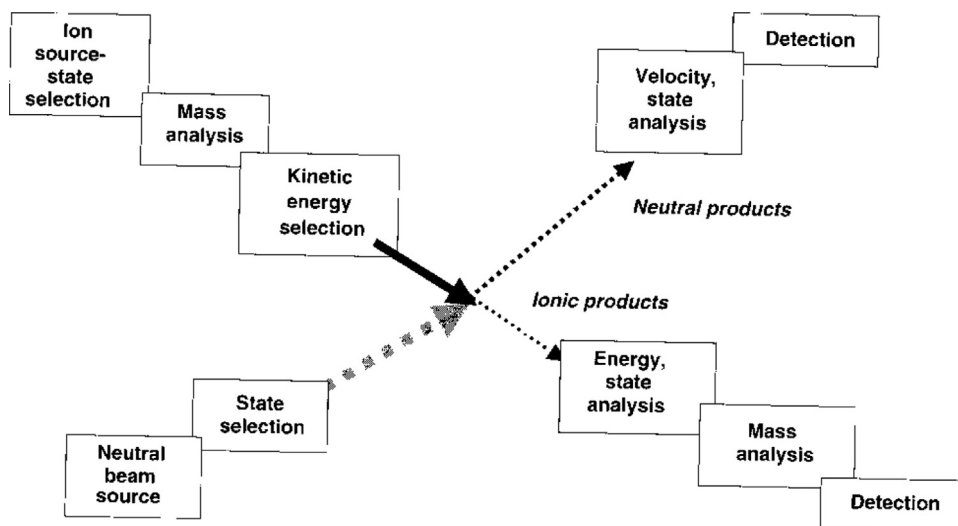


Fig. 1. Schematics of an ideal crossed beam experiment [13].

product ion and neutral product(s) along angular analysis of both. The actual development of instrumentation proceeded gradually to approach this ideal, starting from low-resolution crossed beam devices with mass analysis of the reagent ions beam and angular and velocity (energy) analysis of the product ion.

Because it was the standard technique utilized in mass spectrometry and provided high ion yields, electron impact ionization was used in the first generation crossed-beam instruments. Electronically and vibrationally excited states generated by electron impact could be removed by increasing pressure and by adding quenching gases. Mass selection utilized magnetic sectors or quadrupole mass analyzers. Deceleration of the reagent ions was achieved by multiple-element electrostatic lenses [14–16] and energy selection by cylindrical or hemispherical analyzers [17,18]. For preparation of neutral crossed beams, collimated multichannel effusive sources [14,19] were initially used; later versions utilized supersonic and seeded beams to achieve higher velocity and narrower angular distributions [15,16]. Product ion velocity (or energy analysis) was achieved by simple stopping-potential analyzers [14,20], by electrostatic deflection in cylindrical [16,21] or hemispherical [15,16,22] analyzers or by the time-of-flight method [23]. Mass analysis of product ions utilized magnetic or quadrupole mass analyzers and ions were detected utilizing various kinds of electron multipliers. The position-sensitive coincidence technique introduced early this century [24,25] added the unique capability to detect nascent velocities of product ion pairs originating from dissociation of multiply-charged ions.

Experiments are carried out in the laboratory systems of coordinates (LAB), while dynamical characteristics (angular distributions, relative translational energy distribution of products, comparison with trajectory calculations) are best analyzed in the center-of-mass (CM, barycentric) coordinate system [12,13]. This may be considered as the unique advantage of crossed-beam dynamics experiment. A particularly useful way of analyzing data from these experiments is the Newton velocity diagram [26] (Fig. 2). This figure depicts for a general chemical reaction $A+B \rightarrow C+D$ the relations between laboratory (v) and center-of-mass (u) velocities of reagents and products [12]. The utility of presenting product ion fluxes in the framework of these diagrams, and transformation relations between intensities in the polar laboratory and barycentric coordinate systems or as Cartesian probability units are thoroughly explained in the literature [12,13,27–29]. The utility of Newton diagrams for differentiating reaction mechanisms will become obvious in section 4.

3. Research leaders and key instrumental developments

Because mass spectrometers conventionally involve moderate to high kinetic energy ions, the first dynamics study involved hyperthermal energy ions colliding with neutrals at rest. In these pioneering studies only the translational energy [30,31] or the angular distribution of the ion products [32] was analyzed. Measurement of the translational energy distribution of products was much more informative than angular distributions. In particular, the relatively high velocity of reagent ions at electron volt collision energies impacting a neutral at rest restricts product ion angular distributions to such a narrow forward cone that different velocity components are not resolved. It was clear that the path forward would require measurement of both velocity and scattering angle of products in the next generation of scattering experiments.

Two approaches for measuring both energy (velocity) and angular distributions of product ions were soon developed. A simple scattering chamber was suitable for incident reactant ion energies in the eV range, where the random movement of neutral reagent particles could be neglected relative to the velocity of the ion reagent [17,20–22]. The other approach was the crossed beam technique, where the neutral reagent was formed into a collimated beam to react at the crossing point of this beam with the ion reagent beam [14,15]. With seeded neutral beams and improved

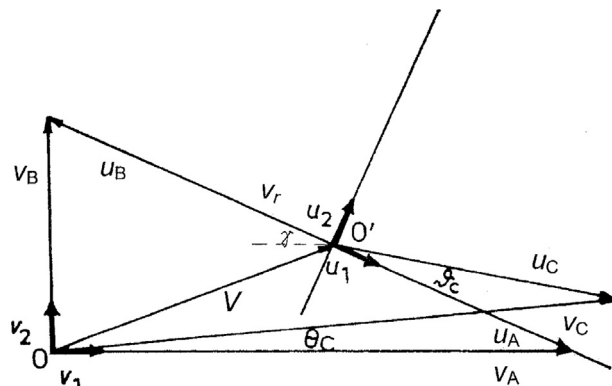


Fig. 2. Newton velocity vector diagram for a reaction $A+B \rightarrow C+D$, showing the relations between laboratory (LAB, v) and center-of-mass (CM, u) quantities [12].

deceleration lenses this approach enabled experiments in which ion and neutral beam velocities are of comparable magnitude.

Early and very powerful single-beam-collision cell machines were introduced in the mid-sixties at Berkeley (B. Mahan's group [22]) and Gainesville (T.L. Bailey's group [21]). In the early seventies generically related single-beam machines were developed in Berlin (A. Henglein's group [20]) and in Baltimore (W.S. Koski's group [17]). The first true crossed-beam apparatus was developed in the mid-sixties at Yale (R. Wolfgang's group [14]) and an improved version of it was created in Prague in early seventies (Z. Herman's group [19]). Crossed beam instruments with additional improvements were built in Kaiserslautern (F. Linder's group [18]), Salt Lake City (J.H. Futrell's group [15]), Rochester (J.M. Farrar's group [16]) and in Freiburg (Teloy, Gerlich [23]). In general, each succeeding apparatus added refinements that did not change the basic research strategy. Important additional information on internal energy exchange in these reactions became available with optical detection of product states in early luminescence experiments carried out by the groups of Ch. Ottinger in Göttingen [33] and J.J. Leventhal at St. Louis [34]. Although electronically excited products are often minor channels of chemical reactions of ions, definitive data on energy disposal in products is important for general understanding of ion–molecule reaction dynamics. More recently the powerful new technique of coincidence detection utilizing a position-sensitive detector has been introduced in London (S.D. Princes's group [24]). A very promising new development is the combination of lasers with position-sensitive detection as carried out by the Weisshaar group [25] in a novel crossed beam apparatus.

4. Early achievements: characterization of reaction mechanisms

One of the first achievements of beam scattering studies was the detailed characterization of two fundamental mechanisms of

ion–molecule reactions—namely, the direct formation of product ions and formation by decomposition of a relatively long-lived intermediate complex. The first mechanism was a prominent feature of exothermic formation of protonated species in collisions of such ions as N_2^+ , Ar^+ , and CO^+ with hydrogen or deuterium. All these reactions exhibited forward scattering of the product ion with respect to the center-of-mass (CM) of the system (Fig. 3). Such direct, impulsive reactions imply a very brief interaction between the reagents in the collision event, comparable to about one vibrational period in the exchanged atom. It may be described as the concerted dissolution of a particular bond in the molecular reagent and formation of a new bond in the molecular product. This feature of the dynamics – energy change as if the reagent ion collided with a quasi-free species that was transferred in the collision – had been characterized earlier by the Henglein group [35] as “spectator stripping” in analogy with the similar mechanism invoked for nuclear reactions [36]. It was commonly assumed that such direct mechanisms would switch to intermediate complex formation at a very low collision energies, but careful experiments showed that direct mechanisms persist even at quasi-thermal collision energies [37] (Fig. 4). This “direct” mechanism was later shown to involve potential energy surfaces that were relatively flat in the region of strongest interaction between the reaction partners. While the stripping model predicted the most probable translational energy release, details of translational energy release and angular scattering clearly indicate that the term “direct” is the preferred description of this mechanism.

The other general class of ion–molecule reactions in which a “persistent intermediate” (long-lived complex) was formed is characterized by scattering of the product ion symmetrically forward and backward with respect to a plane passing through the center-of-mass perpendicular to the relative velocity of the system.

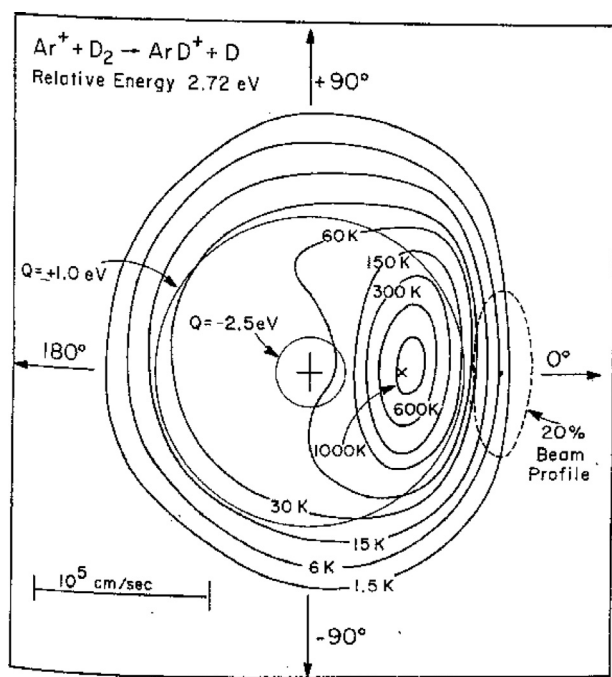


Fig. 3. Scattering diagram of ArD^+ from reaction of Ar^+ with D_2 at the collision energy $T=2.72$ eV. The line $180^\circ-0^\circ$ gives the direction of the relative velocity. Intensity contours show scattering forward with respect to the center-of-mass (cross); dashed-profile of the reagent Ar^+ beam [51].

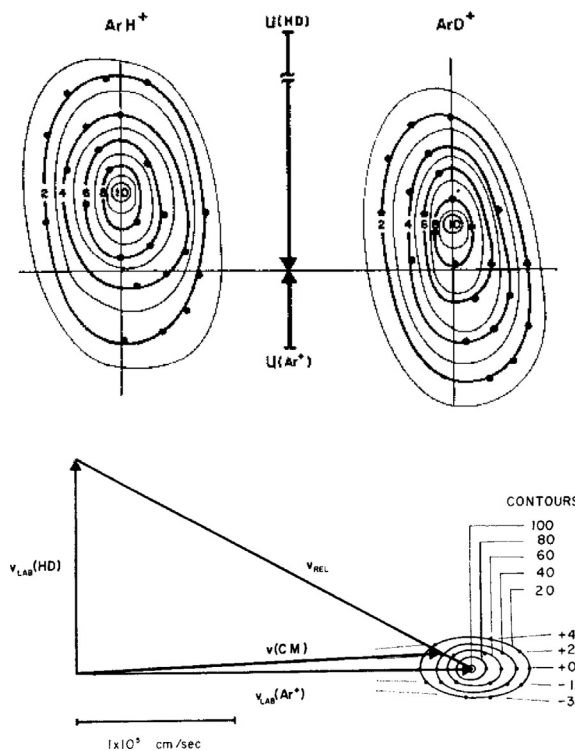


Fig. 4. Upper part: contours of product ion ArH^+ and ArD^+ for reaction $Ar^+ + HD$ at $T=1.31$ eV illustrating forward scattering with respect to the center-of-mass (horizontal line) [28]. Lower part: velocity Newton diagram for reaction $Ar^+ + D_2$ at $T=0.096$ eV with contours of ArD^+ illustrating forward scattering of the product ion even at this very low collision energy [29].

Such a distribution of products implies formation of a collision intermediate in which the constituents stayed within bonding distances for a period of time significantly longer than its period of rotation. This reaction mechanism is often described as a statistical complex in which energy is fully or largely redistributed over the internal degrees of freedom and only a small fraction of total reaction energy (collision energy and reaction exothermicity) is channeled into product translational energy.

Ion–molecule reactions proceeding by such mechanisms were first sought and found in polyatomic systems with many degrees of freedom [38]; they have also been observed in simple three-particle systems that allowed for the formation of a thermodynamically stable intermediate [39] (Fig. 5). The classical model of chemical reactions involving a collision complex with a lifetime long compared to its rotational period [40] correctly describes the product translational energy distribution and how it is influenced by the disposal of the angular momentum [41,42]. The basic concept of the classical model also has its roots in nuclear physics as the “compound nucleus” treatment of the fission process [43].

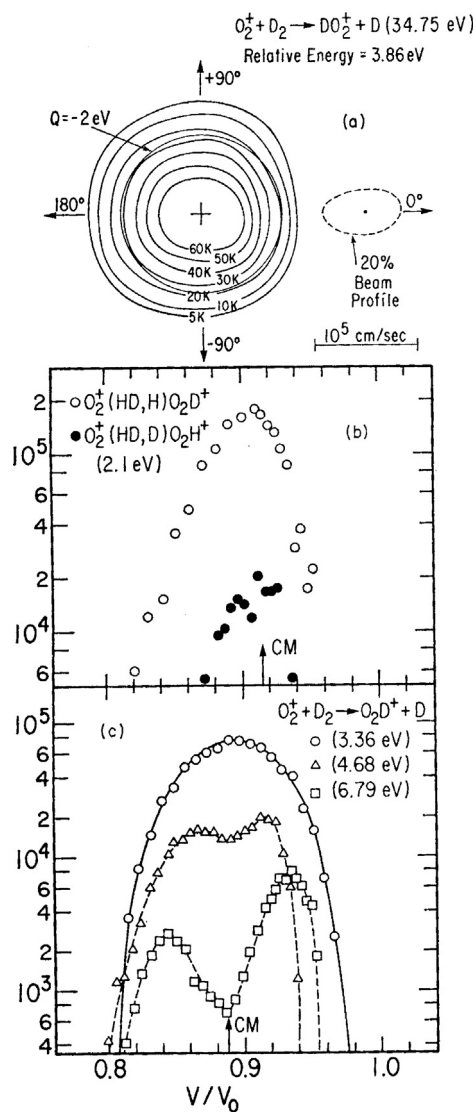


Fig. 5. Contour map of DO_2^+ from reaction of $\text{O}_2^+ + \text{D}_2$ symmetric about the CM (cross), characteristic of the intermediate complex D_2O_2^+ formation. Lower part: velocity profiles of the product ion at different collision energies as indicated. At 6.79 eV the decrease of intensity about the CM shows dissociation of the product ion internally excited above the dissociation limit [49].

Such details as the shape of the rotating complex in its critical configuration and the role of angular momentum have been described [44,45]. Many examples of long-lived complex formation in ion–molecule reactions are now known. Potential energy surfaces defining this mechanism always involve a deep well in the region of reagent interaction, the formation of an intermediate that redistributes energy in this well, and decomposition described by established models for unimolecular decomposition of the rotating species. Systematic studies of reactions of the ions of the first row elements (C^+ , N^+ , O^+ , F^+ , Ar^+) with hydrogen resulting in formation of protonated species in systems $\text{C}^+ + \text{H}_2$ [46,47], $\text{N}^+ + \text{H}_2$ [48], $\text{O}^+ + \text{H}_2$ [49], $\text{F}^+ + \text{D}_2$ [50], $\text{Ar}^+ + \text{D}_2$, [29,37,51], $\text{B}^+ + \text{D}_2$ [52] and further studies of reactions of molecular and polyatomic ions with hydrogen provided large amount of data and specific information defining both direct and intermediate complex formation mechanisms for these systems.

5. Theoretical concepts

Correlation diagrams have provided very useful insights into the electronic states involved in these reactions. By the early seventies computers and quantum chemical computations enabled calculation of relatively accurate potential energy surfaces for the simplest three-particle systems investigated. In particular, the diatomic-in-molecules (DIM) method [53] and its variations provided relatively accurate information on potential energy surfaces for these relatively simple ions [54]. Quasiclassical trajectory studies, performed within the framework of the Born–Oppenheimer approximation, of the three-particle reactions of $\text{D}^+ + \text{HD}$ [55] and $\text{H}_2^+ + \text{He}$ [56], were early examples. Since chemical reactions of ions are very often accompanied by charge transfer processes, multiple potential energy surfaces and non-adiabatic effects are quite important. An efficient method for trajectory calculations on crossing potential energy surfaces is the trajectory-surface-hopping method (THS) [57] which has been applied successfully to many reaction systems. Enormous advances in theoretical approaches during this century and accompanying advances in computer techniques and computing power have completely changed the theoretical landscape but will not be described in our short review.

6. Dynamics of electron transfer (charge transfer) reactions

An early theoretical study of non-adiabatic electron transfer and chemical reaction for $\text{Ar}^+ + \text{H}_2$ collisions [58] was the motivation for a crossed-beam study of this system. Theory predicted that a minor reaction channel, the charge exchange product H_2^+ , would be scattered essentially parallel to the initial H_2 velocity vector with translational energy release corresponding to formation of specific vibrational states closest to resonance. Although formation of the major reaction product, ArH^+ , was well studied, the electron transfer channel had not been characterized. The experimental study [59] fully confirmed the predictions of the theoretical study and also detected modest backward scattering from close collisions exhibiting a significant range of energy transfer and correspondingly broad range of H_2^+ internal states. The same principle – that internal states of the polyatomic product ion closest in resonance with the recombination energy of the reagent ion are highly favored – was also observed for polyatomic neutrals in the system $\text{Kr}^+ + \text{CH}_4$ [60].

The charge-transfer reaction $\text{Ar}^+ + \text{N}_2$ is a well-studied system, both experimentally and theoretically [10,61,62]. Fig. 6 illustrates the resolved population of several N_2^+ vibrational states in a 0.78 eV collision energy crossed-beam experiment. This rather complex scattering diagram exhibits a strongly peaked N_2^+ , $v=1$ peak that is forward scattered (with respect to the N_2 neutral

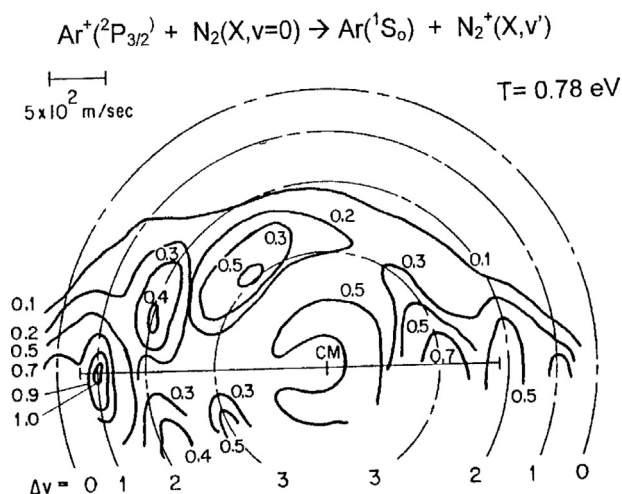


Fig. 6. Scattering diagram of N_2^+ from the electron exchange reaction $Ar^+ + N_2$ at $T = 0.78$ eV. Concentric cycles about the CM indicate velocities of the product ion if formed in the respective vibrational states [10,61].

beam) along with extensive angular scattering populations of $v = 2$ and $v = 3$ states. Clearly the scattering dynamics for this simple system are strongly influenced by the details of potential energy surface.

7. Dynamics of reactions of negative ions

Scattering studies of anion chemical reactions were initiated about a decade later than reactions of cations. The reaction of oxygen negative ion O^- and hydrogen leading to OH^- was investigated in a low-resolution crossed-beam experiment at moderate collision energy in the early seventies [63,64]. With improved instrumentation, Farrar's group [65] later resolved product vibrational states over a broad range of collision energies and reported a rather complex dependence of dynamics on collision energy. Involvement of several potential energy surfaces with rather shallow energy wells rationalized the findings of non-statistical product internal state distributions. A high-quality *ab initio* potential surface [66] provided motivation for more recent studies of this system [67].

Scattering beam studies of the reaction of O^- with HF giving OH and F^- [68] showed forward-backward scattering of the products at low collision energies – less than 1 eV – implying formation of an intermediate complex generating neutral OH in vibrational states $v = 0, 1$ (Fig. 7). Classical trajectory studies of this system [69] demonstrated that the reaction proceeds via an intermediate complex. A crossed-beam investigation of the reaction of O^- with H_2O leading to $OH^- + OH$ [70] revealed rather complex dynamics, formation of an intermediate complex, rebound-scattering near threshold, and stripping scattering at collision energies above 1 eV. Additional information on dynamics of chemical reactions of negative ions is available from non-beam experiments, including mass spectrometric, flow tube, guided beam, photoelectron spectroscopy, state-selected reagent and laser-induced fluorescence techniques [11].

8. Selected specific studies

8.1. The “simplest” chemical reaction, $H^+ + H_2$

This “simplest” chemical reaction (three atoms, two electrons) was an early target of scattering beam studies. All possible

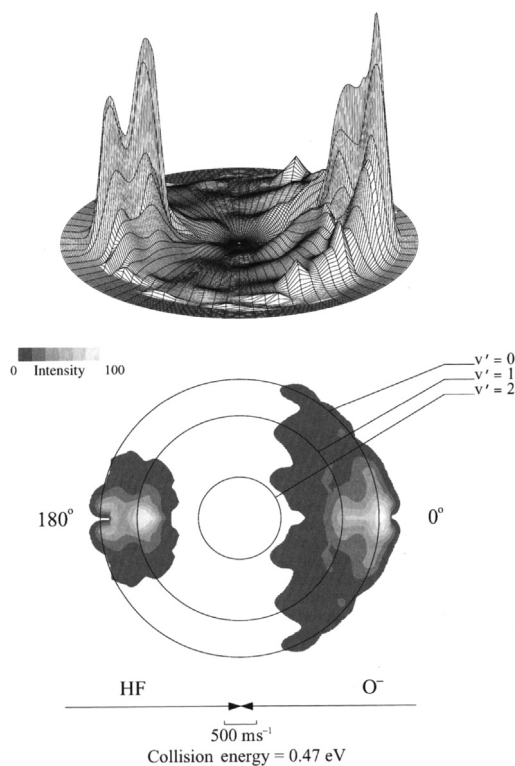


Fig. 7. Three-dimensional scattering diagram of F^- from reaction between O^- and HF at the collision energy of 0.47 eV, indicating a long-lived complex formation. Specific vibrational states of OH, as determined by momentum conservation, are labelled by their quantum numbers [13,68].

processes in the systems $H^+ + D_2$ and $D^+ + HD$ (nuclear rearrangement, charge transfer, dissociation) were investigated over the range of collision energies 1–7 eV [71]. The results were interpreted on the basis of a model based on trajectory calculations propagated on a diatomics-in-molecules surface in which non-adiabatic effects were treated using the trajectory-surface-hopping method. An important feature of their theoretical treatment was splitting the potential surface at an avoided surface crossing at about 2 eV with a seam that separates processes occurring on the lower surface with a deep potential well (formation of H_3^+ complex) from those occurring on the upper repulsive surface (which is rather similar to that of the neutral H_3 system). Quite good agreement between experimental results and trajectory calculations was demonstrated [71].

This study inspired a subsequent high-resolution study of the formation of D^+ in the reaction $H^+ + D_2$ at collision energies below the potential surface seam that utilized a differential scattering apparatus with guided beams and time-of-flight detection of products [23,72]. Energy profiles resolved the vibrational and rotational states distribution of D^+ with sufficient resolution to enable detailed comparison with theoretical simulations obtained by the most-dynamically-based (MDB) variation of the statistical model [73]. Excellent agreement between the experiments and calculations on the population of product internal states was obtained (Fig. 8), strongly supporting the concept that reactions occurring on the lower surface proceed via a statistically randomized HD_2^+ intermediate complex. This pioneering study of H_3^+ as a test example initiated a series of theoretical papers on decomposition of small complexes [74]. A recent theoretical investigation compares the previous experimental results with results of quantum mechanical, quasiclassical trajectory, and statistical quasiclassical trajectory calculations [75].

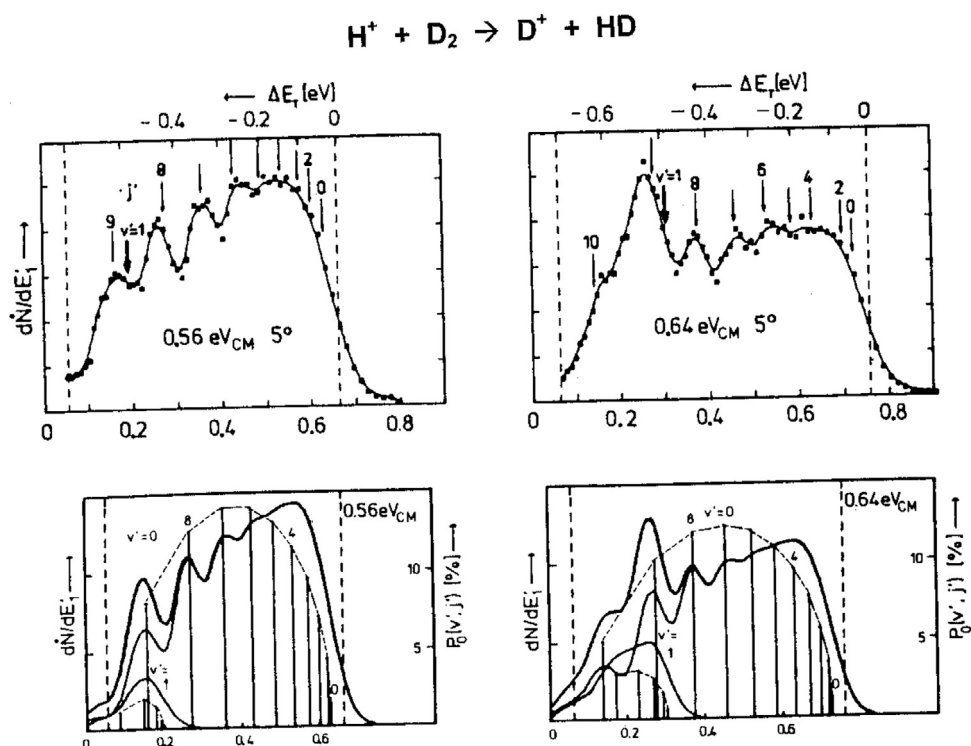


Fig. 8. Energy profiles of D^+ (LAB scattering angle 5°) from reaction $\text{H}^+ + \text{D}_2$ at the collision energies 0.56 eV (left) and 0.64 eV (right) with arrows pointing to the positions of vibrational (ν) and rotational (j) levels of HD formed. Lower part: comparison of the experimental data with the results of MDB calculations (sticks and dashed line) [72].

8.2. Parallel mechanisms in ion–molecule reactions

The reaction between the methane molecular cation, CH_4^+ , and methane molecule is among the first and most-studied ion–molecule reactions [76]. The dynamics of this “simple” reaction is rather complicated. A scattering study of CH_5^+ formation provided evidence for several parallel mechanisms [77] (Fig. 9). They were formally classified as (a) direct proton transfer from CH_4^+ to CH_4 characteristic of a stripping mechanism; (b) direct H-atom transfer from neutral CH_4 to the cation CH_4^+ with an energy release also following the stripping mechanism; and (c) decomposition of the intermediate (C_2H_8^+) collision complex exhibiting modest energy release, implying dissociation of a statistical complex. The relative weights of these mechanisms changed as a function of both collision and internal energy of CH_4^+ [78]. A theoretical study [79] fully rationalized the occurrence of these three mechanisms. Analogous complex dynamics have been observed, with variations in the relative contribution of the particular mechanisms, in molecular ion–molecule reactions of other small molecule systems: e.g. water, acetonitrile, methanol etc.

8.3. Hydride ion transfer

Hydride-ion transfer reactions are prominent ion–molecule reaction products in saturated hydrocarbons and represent a class of reactions important in many areas of chemistry. The dynamics of H^- transfer in reactions of CD_3^+ with ethane (formation of C_2H_5^+ and $\text{C}_2\text{H}_2\text{D}_3^+$) [80] and methane (formation of CH_3^+ and CD_2H^+) [81] were investigated in scattering experiments. The results indicated formation of a short-lived protonated carbonium ion complex (mean lifetime of 10^{-12} s or less) that involved formation of a non-classical, three-center, two-electron bond. Hydrogen–deuterium exchange along the protonated hydrocarbon chain rationalized the formation of the partially deuterated products, formally classified as products of methylene transfer. A parallel

guided-beam study [82] demonstrated that the fraction of very low laboratory energy product ions scattered in the direction of the neutral reagent was underestimated in those experiments, indicating an even shorter mean lifetime of the intermediate complex.

8.4. Ion–molecule reaction in both directions: $\text{H}_3^+ + \text{Ar}$ and $\text{ArH}^+ + \text{H}_2$ systems

Two reactions, the reaction of H_3^+ with Ar leading to $\text{ArH}^+ + \text{H}_2$, endothermic by about 0.6 eV, and the reverse exothermic reaction were studied in a crossed beam experiment [83] that provided a unique opportunity to investigate a chemical reaction occurring in both directions. Both reactions were found to proceed by a direct proton transfer mechanism over the entire collision energy range (0.87–9.7 eV, and 0.18–6.7 eV, respectively). Rather remarkably, these dynamic features were rationalized in terms of a modified elastic spectator model that invoked proton stripping at the hard-sphere collision radius [84] with only minor deviations at the lowest collision energy.

8.5. Mechanisms and energy disposal with vibrationally-specified reactants: the $(\text{C}_2\text{H}_2\text{--OCS})^+$ system

Electron transfer in both directions ($\text{C}_2\text{H}_2^+ + \text{OCS}$ and $\text{OCS}^+ + \text{C}_2\text{H}_2$) and S-atom transfer were investigated in an extensive study of this system, the first dynamics investigation of the role of vibrational modes for polyatomic ions [85]. Multi-photon ionization was used to prepare C_2H_2^+ in the ground and $\nu_2=1$ and 2 vibrational levels, and OCS^+ in the ground and two specified excited vibrational levels. The guided-beam technique, operated with guided field moderation [6], in combination with a supersonic crossed beam was used to obtain the scattering data. The electron transfer reactions were found to proceed by very different mechanisms. For the exothermic $\text{C}_2\text{H}_2^+ + \text{OCS}$ reaction the

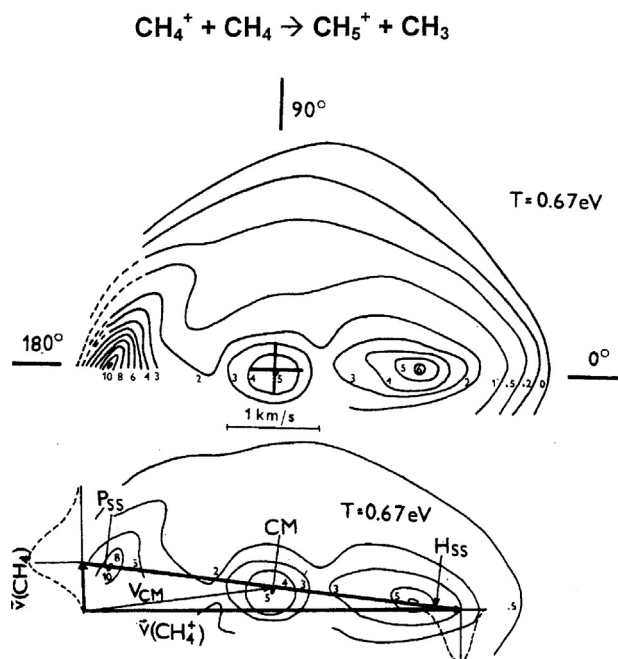


Fig. 9. Contour scattering diagram of CH_5^+ (upper part) from reaction $\text{CH}_4^+ + \text{CH}_4$ at the collision energy of 0.67 eV, and the respective Newton diagram with simplified version of contours and beam velocity spreads, indicating the parallel mechanisms of product formation (P_{SS} -direct proton transfer, H_{SS} -direct H-atom transfer, complex formation (about CM) [77].

dominant mechanism was long-range electron hopping, while the $\text{OCS}^+ + \text{C}_2\text{H}_2$ (endothermic by 0.23 eV) involved intimate direct collisions promoted by vibrational excitation at low collision energies. Chemical reactions leading to $\text{C}_2\text{H}_2\text{S}^+$ proceeded prevalently by two distinct direct mechanisms for both C_2H_2^+ and OCS^+ – specifically described as glancing/stripping and rebound – that were strongly influenced by collision energy and vibrational excitation. Complex formation was an important mechanism at collision energies lower than 0.5 eV.

9. Reactions of dications: Coulomb effects in electron transfer and chemical reactions

Reactive collisions of doubly-charged ions have been investigated since the early eighties. The main reaction channel at high incident energies, studied primarily by physicists, was single-electron transfer to form two singly-charged product ions that recoiled from each other. Measurement of translational energy release resulting from Coulomb repulsion between the two product ions accurately defined the electronic states of the species involved (translational energy spectroscopy). Cross-sections of these reactions are defined by the “reaction window” concept. Following Landau–Zener formalism, adiabatic transitions between the reagent and product potential energy states are efficient only in a certain range of internuclear distances. Depending on collision energy, this region is in the range 2–6 Å, corresponding to exothermicities of electron transfer reactions of 2.5–7 eV.

Scattering experiments at eV collision energies with the simple atomic ion–atom system $\text{Ar}^{2+} + \text{He}$ [86] exhibited preferential forward scattering of the product ion Ar^+ with a differential cross section, whose shape closely matched that was predicted by theoretical calculations [87,88]. For simple molecular systems, combination of beam results with product luminescence studies [89] made it possible to determine the partitioning of energy between product translation, vibration, and rotation [90].

Chemical reactions of doubly-charged ions were first suggested [91] and reported for metal dications in flow-tube [92] and Fourier transform ion cyclotron resonance (FT-ICR) experiments [93] and later extended to include molecular dications [94]. The latter experiments motivated a series of beam scattering experiments of molecular dications with hydrogen that generated the protonated molecular cation and a proton as products. Observation of a facile proton transfer in chemical reactions of molecular dications containing hydrogen, pointed to a rather new type of general reactions [95]. Chemical reactions were in all cases accompanied by a strong channel of charge transfer and by dissociative processes. Both direct mechanisms (e.g., $\text{CF}_2\text{D}^+ + \text{H}^+$ in $\text{CF}_2^{2+} + \text{H}_2$ collisions [96]) and complex formation (e.g., $\text{CO}_2\text{D}^+ + \text{H}^+$ in $\text{CO}_2^{2+} + \text{H}_2$ collisions [97]) were observed for the reaction products. Some, but not all, of the dissociative product channels result from further decomposition of internally excited product ions. This was demonstrated for several systems in more advanced crossed-beam studies utilizing position-sensitive coincidence detection of product ions [98]. Bond-forming reactions of triply-charged cations with neutral molecules have also been described [99].

A simple general model for reactions of dications, based on crossing of potential energy terms, was developed [96] that rationalized the relative importance of different competing processes: (a) electron transfer processes leading to two singly-charged ions; (b) chemical reactions leading to two singly-charged chemically distinct product ions; and (c) chemical reactions leading to doubly-charged, chemically distinct product ions and a neutral product. The latter class of reactions, initially observed as a very minor reaction channel [100], becomes more important for large hydrocarbon dications. A class of reactions between aromatic dications (like $\text{C}_7\text{H}_6^{2+}$, $\text{C}_7\text{H}_7^{2+}$, $\text{C}_7\text{H}_8^{2+}$ from toluene) and acetylene [101] or methane [102] demonstrated the importance of type (c) reactions; for these systems a neutral hydrogen molecule was eliminated and a dication with a longer carbon chain was formed.

10. Dynamics of collision-induced dissociation

Collision-induced dissociation (CID) of polyatomic ions in tandem mass spectrometry has become an important analytical tool utilized by organic and bioorganic mass spectrometrists, as described elsewhere in this Special Issue by Graham Cooks and Keith Jennings. That impulsive collisions are involved in the conversion of kinetic to internal energy in CID was suggested by the reported dependence of fragmentation patterns of keV energy polyatomic organic ions on scattering some 35 years ago [103]; general mechanisms for moderate to high energy CID were well established by the beginning of this century [104].

The first true crossed-beam study of collision-induced dissociation of a polyatomic ion at eV collision energies in which the final energy and scattering angle of dissociation products were measured was a study of methane and propane molecular ions in the mid-eighties [105]. As anticipated for impulsive collisions, the amount of energy transferred into the ion increased with scattering angle and the degree of dissociation was directly correlated with internal excitation of the recoiling projectile ion. For polyatomic ions of moderate complexity, vibronic excitation of recoiling ions is followed by rapid intramolecular relaxation to the ground state; unimolecular dissociation of the ground state is well-described by RRKM kinetics [106]. Because impulsive collisions explore the closely-spaced repulsive part of potential hyper-surfaces, dissociation from excited states sometimes occurs; this mechanism is particularly pronounced in acetone, whose CID at sub-eV collision energy is dominated by back-scattered ions that have gained 2.2 eV in translational energy, the distinctive signature of the $X \leftarrow A$ transition triggered by a repulsive collision [107,108].

11. Ion-surface collision dynamics

Interest in the interactions between hyperthermal ions and surfaces has grown steadily over the last twenty years. In structural mass spectrometry, in particular, surface collision activation is increasingly used as a well-defined means for selectively dissociating polyatomic organic (bioorganic), polymeric, and cluster ions [109–114]. Surface-induced dissociation (SID) shares many characteristics in common with CID activation. The remarkable utility of the technique reflects its ability to deposit in a very controlled fashion either relatively small amounts or relatively large amounts or a range of internal energy in the projectile ion by varying the nature of the surface and the kinetic energy and angle of incidence of the impacting ion.

Scattering experiments have provided a deeper insight into the elementary processes involved in ion-surface collisions of polyatomic ions, including detailed dynamics of energy transfer and energy partitioning in ion-surface interactions. A few studies of SID dynamics of molecular ions of small organic molecules colliding with well characterized surfaces have been conducted with specially designed instruments [115] or by replacing the neutral beam source with a surface [116]. These instruments enabled measurement of the identity of product ions scattered from the surface, their translational energy and angular distributions as a function of incident energy and angle of the projectile ions.

Not unexpectedly, the outcome of ion-surface collisions depends strongly on the nature of the projectile ion, collision energy, angle of incidence, and composition of the surface; species adsorbed on the surface also modify the dynamics. Ion neutralization, the dominant process in all cases, is of least interest to chemists. Other processes – landing of intact ions, reactions on the surface, SID – vary by orders of magnitude, depending primarily on the nature of the surface and the colliding ion [114,117]. Survival probabilities of different ions on room-temperature, hydrocarbon-covered metal and carbon surfaces and on heated surfaces (devoid of hydrocarbons) of several metals and carbon have been measured and a correlation with the recombination energy (ionization energy) of the ion was established [117]. Early SID experiments utilized stainless steel surfaces adventitiously coated with low vapor pressure hydrocarbons and most recent experiments employ much better-defined self-assembled-monolayer (SAM) surfaces. Studies of low energy collisions of small polyatomic ions with SAM surfaces of different composition have established general features of SID dynamics [113,115]. Teflon-like perfluorocarbon F-SAM's are especially effective SID surfaces, exhibiting the highest efficiency of energy transfer and ion survivability, of the order of 20% for carefully prepared 12-carbon alkyl thiols self-assembled on planar gold substrates. [115].

Analogous to CID, the dominant mechanism of surface-induced dissociation in impulsive collisions with the neutral collision partner is internal excitation of the recoiling ion, followed by unimolecular dissociation of the activated ion [116,119–121]. Fig. 10 is a scattering diagram adapted for ion-surface collisions that further elaborates this analogy. It displays the results of a detailed scattering study of collisions of ethanol cations (incident energy 28.9 eV and incident angle 45°) with a SAM surface generated by the self-assembly reaction of $\text{CF}_3(\text{CF}_2)_9(\text{CH}_2)_2\text{SH}$ with the 111 surface of a gold crystal [115]. This diagram depicts an incoming ion beam impacting the F-SAM surface at 45° and constructs an elastic scattering circle corresponding to zero energy exchange in the collision. By requiring the maxima of all the observed CH_2OH^+ product ions to fall on a circle one can determine the mass of the scattering entity generating this scattering pattern. Using the operative equations described previously, the data plotted in Fig. 10 are consistent with scattering by a particle effective mass of about 117 amu. That this mass essentially matches that of the

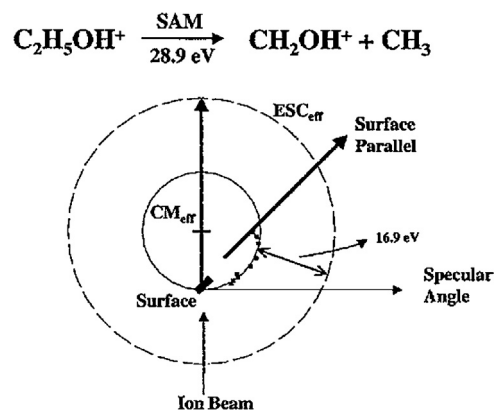


Fig. 10. Modified Newton diagram for collision of $\text{C}_2\text{H}_5\text{OH}^+$ with a perfluorohydrocarbon-SAM surface demonstrating that most probable velocities of fragment ions follow a circle (CM_{eff}) that fall on the post-collision velocity vector. This circle implies that the excited projectile ion collides with an effective mass of the SAM surface of 117 daltons [115].

terminal C_2F_5 group (119 amu) or 6 fluorine atoms (114 amu) implies that prompt recoil scattering involves, to a first approximation, terminal group(s) of the F-SAM chain or clusters of atoms at the surface. This inference – that dynamics is dominated by collision with a cluster of atoms on the surface – is supported by a more detailed study of energy partitioning in SID of ethanol cations [118], other polyatomic ions [116] and with theoretical predictions [122,123]. Classical trajectory studies of polyatomic ion collisions with an ideal F-SAM surface that treats the $-\text{CF}_3$ and $-\text{CF}_2$ groups as united atoms describe the effective scattering entity as a small ensemble of near surface “atoms” governing the partitioning of projectile translational energy into vibrational modes of the surface and internal and translational energy of the recoiling ion; this accounts for the strong mass effect seen both experimentally and theoretically [123].

12. Concluding remarks

This brief summary of roughly four decades of study has demonstrated that ion-neutral collision dynamics exhibits all the nuances of neutral-neutral reaction dynamics that were the inspiration for studies of these reactions utilizing molecular beam techniques. The added characteristic that one of the reagents is charged either positively or negatively is a feature that influences reaction mechanisms and also enables detailed investigation of high energy collisions and low probability reaction channels. For the authors it has been an exciting voyage of discovery that has unraveled mysteries and advanced our understanding of fundamentals of ion-molecule chemistry.

References

- [1] E.H. Taylor, S. Datz, *J. Chem. Phys.* 23 (1955) 1711.
- [2] D.R. Herschbach, *Adv. Chem. Phys.* 10 (1966) 332.
- [3] J.H. Futrell, T.O. Tienan, in: J.L. Franklin (Ed.), *Ion-Molecule Reactions*, 2, Plenum Press, New York, 1972, pp. 485 0-306-30552-6.
- [4] D. Gerlich, *The Encyclopedia of Mass Spectrometry*, (in: M.L. Gross, R. Caprioli, Eds.), Vol. 1 (P.B. Armentrout, Volume Ed.), Elsevier, 2003; (ISBN 0-08-043802-4), 158–173.
- [5] W.R. Gentry, *The Encyclopedia of Mass Spectrometry*, (in: M.L. Gross, R. Caprioli, Eds.), Vol. 1 (P.B. Armentrout, Volume Ed.), Elsevier, 2003; (ISBN 0-08-043802-4), 174–182.
- [6] S. Mark, D. Gerlich, *Chem. Phys.* 209 (1996) 235.
- [7] Z. Herman, R. Wolfgang, in: J.L. Franklin (Ed.), *Ion-Molecule Reactions*, 2, Plenum Press, New York, 1972, pp. 553 0-306-30552-6.
- [8] W.S. Koski, *Adv. Chem. Phys.* 30 (1975) 185.
- [9] W.R. Gentry, in: M. Bowers (Ed.), *Gas Phase Ion Chemistry*, 2, Academic Press, New York, 1979, pp. 221–293.
- [10] J.H. Futrell, *Adv. Chem. Phys.* 82 (1992) 523.

- [11] J.M. Farrar, *Annu. Rev. Phys. Chem.* 45 (1995) 525.
- [12] Z. Herman, *Int. J. Mass Spectrom.* 212 (2001) 413.
- [13] J.M. Farrar, *The Encyclopedia of Mass Spectrometry*, (in: M.L. Gross, R. Caprioli, Eds.), Vol. 1 (P.B. Armentrout, Volume Ed.), Elsevier, 2003; (ISBN 0-08-043802-4). 158–173.
- [14] Z. Herman, J.D. Kerstetter, T.L. Rose, R. Wolfgang, *Rev. Sci. Instr.* 40 (1969) 538.
- [15] C.R. Blakely, P.W. Ryan, M.I. Vestal, J.H. Futrell, *Rev. Sci. Instr.* 47 (1974) 15.
- [16] R.M. Bilotta, F.N. Preuninger, J.M. Farrar, *J. Chem. Phys.* 73 (1980) 1637.
- [17] K.I. Wendel, C.A. Jones, J.J. Kaufman, W.S. Koski, *J. Chem. Phys.* 63 (1975) 750.
- [18] V. Hermann, H. Schmidt, F. Linder, *J. Phys. B* 11 (1978) 493.
- [19] Z. Herman, K. Birkinshaw, *Ber. Bunsenges Phys. Chem.* 77 (1973) 566.
- [20] G. Bosse, A.A. Ding, Henglein, *Ber. Bunsenges Phys. Chem.* 75 (1971) 413.
- [21] R.L. Champion, L.D. Doverspike, T.L. Bailey, *J. Chem. Phys.* 45 (1966) 4377.
- [22] W.R. Gentry, E.A. Gislason, Y.-T. Lee, B.H. Mahan, C.-W. Tsao, *Disc. Faraday Soc.* 44 (1968) 3058.
- [23] E. Teloy, D. Gerlich, *Chem. Phys.* 4 (1974) 417.
- [24] W.-P. Wu, S.M. Harper, S.D. Price, *Meas. Sci. Technol.* 13 (2002) 1512.
- [25] E.L. Reichert, J.C. Weisshaar, *J. Phys. Chem. A* 106 (2002) 5563.
- [26] D.R. Herschbach, *Discuss. Faraday Soc.* 33 (1962) 149.
- [27] R. Wolfgang, J.R. Cross, *J. Phys. Chem.* 73 (1969) 743.
- [28] B. Friedrich, Z. Herman, *Collection Czech. Chem. Commun.* 49 (1984) 570.
- [29] P.M. Hierl, Z. Herman, R. Wolfgang, *J. Chem. Phys.* 53 (1970) 660.
- [30] A. Henglein, K. Lacmann, G. Jacobs, *Ber. Bunsenges Phys. Chem.* 69 (1965) 279.
- [31] K. Lacmann, A. Henglein, *Ber. Bunsenges Phys. Chem.* 69 (1965) 292.
- [32] B.R. Turner, M.A. Fineman, R.F. Stebbings, *J. Chem. Phys.* 42 (1965) 4088.
- [33] Ch. Ottinger, in: M. Bowers (Ed.), *Gas Phase Ion Chemistry*, 3, Academic Press, New York, 1984, pp. 249.
- [34] J.J. Leventhal, in: M. Bowers (Ed.), *Gas Phase Ion Chemistry*, 3, Academic Press, New York, 1984, pp. 309.
- [35] K. Lacmann, A. Henglein, B. Knoll, *J. Chem. Phys.* 43 (1965) 1048.
- [36] B.L. Cohen, A.G. Rubin, *Phys. Rev.* 114 (1959) 1143.
- [37] Z. Herman, J.D. Kerstetter, T.L. Rose, R. Wolfgang, *Discuss. Faraday Soc.* 44 (1967) 123.
- [38] Z. Herman, A. Lee, R. Wolfgang, *J. Chem. Phys.* 51 (452) (1969).
- [39] E.A. Gislason, B.H. Mahan, C.-W. Tsao, A.S. Werner, *J. Chem. Phys.* 50 (1969) 5418.
- [40] W.B. Miller, S.A. Safran, D.R. Herschbach, *Discuss. Faraday Soc.* 44 (1967) 108.
- [41] A. Lee, R.I. LeRoy, Z. Herman, R. Wolfgang, *J.C. Tully, Chem. Phys. Lett.* 12 (1972) 589.
- [42] C.E. Klots, J. Polach, *J. Phys. Chem.* 99 (1995) 15396.
- [43] I. Halpern, *Ann. Rev. Nucl. Sci.* 9 (1959) 245.
- [44] M. Sadílek, Z. Herman, *J. Phys. Chem.* 97 (1993) 2147.
- [45] J. Žabka, Z. Dolejšek, J. Hrušák, Z. Herman, *Int. J. Mass Spectrom.* 185–187 (1999) 195.
- [46] B.H. Mahan, T.M. Sloane, *J. Chem. Phys.* 59 (1973) 5661.
- [47] C.A. Jones, K.I. Wendell, W.S. Koski, *J. Chem. Phys.* 66 (1976) 5325.
- [48] B.H. Mahan, W.H.F. Ruska, *J. Chem. Phys.* 65 (1976) 5044.
- [49] K.T. Gillen, B.H. Mahan, J.S. Winn, *J. Chem. Phys.* 58 (1973) 5373.
- [50] C.A. Jones, I. Sauer, J.J. Kaufman, W.S. Koski, *J. Chem. Phys.* 67 (1977) 3599.
- [51] M. Chiang, E.A. Gislason, B.H. Mahan, C.W. Tsao, A.S. Werner, *J. Chem. Phys.* 52 (1970) 2698.
- [52] B. Friedrich, Z. Herman, *Chem. Phys.* 69 (1982) 433.
- [53] O. Ellison, *J. Am. Chem. Soc.* 85 (1963) 3540.
- [54] J.C. Tully, *J. Chem. Phys.* 58 (1973) 1396.
- [55] R.K. Preston, J.C. Tully, *J. Chem. Phys.* 54 (1971) 4297.
- [56] F. Schneider, U. Havemann, L. Züllicke, V. Pacák, K. Birkinshaw, Z. Herman, *Chem. Phys. Lett.* 37 (1976) 323.
- [57] R.K. Preston, J.C. Tully, *J. Chem. Phys.* 55 (1971) 562.
- [58] S. Chapman, R.K. Preston, *J. Chem. Phys.* 60 (1974) 650.
- [59] P.M. Hierl, V. Pacák, Z. Herman, *J. Chem. Phys.* 67 (1977) 2678.
- [60] Z. Herman, B. Friedrich, *J. Chem. Phys.* 102 (1995) 7017.
- [61] K. Birkinshaw, A. Shukla, S. Howard, J.H. Futrell, *Chem. Phys.* 113 (1987) 149.
- [62] E.A. Gislason, G. Parlant, M. Sizun, in: M. Baer, C.Y. Ng (Eds.), *State-Selected and State-to-State Ion–molecule Reaction Dynamics*, Part 2, John Wiley, New York, 2014, pp. 321.
- [63] E. Herbst, L.G. Payne, R.L. Champion, L.D. Doverspike, *Chem. Phys.* 42 (1979) 423 and references therein.
- [64] S.G. Johnson, L.N. Kremer, C.J. Metral, R.J. Cross, *J. Chem. Phys.* 68 (1978) 1444.
- [65] M.A. Carpenter, M.T. Zanni, J.M. Farrar, *J. Phys. Chem.* 99 (1995) 1380.
- [66] H.-J. Werner, U. Mänz, P. Rosmus, *J. Phys. Chem.* 87 (1987) 2913.
- [67] Y. Li, L. Liu, J.M. Farrar, *J. Phys. Chem. A* 113 (2009) 15233.
- [68] D.J. Levandier, D.F. Varley, M.A. Carpenter, J.M. Farrar, *J. Chem. Phys.* 99 (1993) 148.
- [69] H. Tachikawa, H. Takamura, H. Yoshida, *J. Phys. Chem.* 98 (1994) 5298.
- [70] D.F. Varley, D.J. Levandier, J.M. Farrar, *J. Chem. Phys.* 96 (1992) 8806.
- [71] J.R. Krenos, R.K. Preston, R. Wolfgang, J.C. Tully, *J. Chem. Phys.* 60 (1974) 1634.
- [72] D. Gerlich, *Adv. Chem. Phys.* 82 (1992) 1.
- [73] D. Gerlich, U. Nowotny, Ch. Schlier, E. Teloy, *Chem. Phys.* 47 (1980) 245.
- [74] E. Pollak, Ch. Schlier, *Acc. Chem. Res.* 22 (1989) 223.
- [75] P.G. Jambrina, J.M. Alvarino, D. Gerlich, M. Hankel, V.J. Herrero, V. Sáez-Rábanos, F.J. Aoiz, *Phys. Chem. Chem. Phys.* 14 (2012) 3346.
- [76] V.L. Talroze, A.A. Ljubimova, *Dokl. Akad. Nauk SSSR* 86 (1952) 909.
- [77] Z. Herman, M.J. Henchman, B. Friedrich, *J. Chem. Phys.* 93 (1990) 4916.
- [78] Z. Herman, K. Tanaka, T. Kato, I. Koyano, *J. Chem. Phys.* 85 (1986) 5705.
- [79] K. Kamiya, K. Morokuma, *Chem. Phys. Lett.* 123 (1986) 331.
- [80] M. Fárník, Z. Dolejšek, Z. Herman, V.E. Bondybey, *Chem. Phys. Lett.* 216 (1993) 458.
- [81] J. Žabka, M. Fárník, Z. Dolejšek, J. Polách, Z. Herman, *J. Phys. Chem.* 99 (1995) 15595.
- [82] S. Mark, C. Schellhammer, G. Niedner-Schattenburg, D. Gerlich, *J. Phys. Chem.* 99 (1995) 15594.
- [83] C.R. Blakely, M.L. Vestal, J.H. Futrell, *J. Chem. Phys.* 66 (1977) 4111.
- [84] M.L. Vestal, A.L. Wahrhaftig, J.H. Futrell, *J. Phys. Chem.* 80 (1976) 2892.
- [85] Y.-H. Chiu, H. Fu, J.-T. Huang, S.L. Anderson, *J. Chem. Phys.* 105 (1996) 3089.
- [86] B. Friedrich, Z. Herman, *Chem. Phys. Lett.* 107 (1984) 375.
- [87] B. Friedrich, Š. Pick, L. Hládek, Z. Herman, E.E. Nikitin, A.I. Reznikov, S.Ya. Umanskiy, *J. Chem. Phys.* 84 (1986) 807.
- [88] J.P. Braga, D.B. Knowles, J.N. Murrell, *Mol. Phys.* 57 (1986) 665.
- [89] A. Ehbrecht, N. Mustafa, Ch. Ottinger, Z. Herman, *J. Chem. Phys.* 105 (1996) 9836.
- [90] Z. Herman, *Mol. Phys.* 111 (2013) 1697.
- [91] K.G. Spears, F.C. Fehsenfeld, F. Mc Farland, E.E. Ferguson, *J. Chem. Phys.* 56 (1972) 2562.
- [92] J.C. Weisshaar, *Acc. Chem. Res.* 26 (1993) 213.
- [93] L.M. Roth, B.S. Freiser, *Mass. Spectrom. Revs.* 10 (1991) 303.
- [94] S.D. Price, M. Manning, S.R. Leone, *J. Am. Chem. Soc.* 116 (1994) 8673.
- [95] J. Roithová, Z. Herman, D. Schröder, H. Schwarz, *Chem. Eur. J.* 12 (2006) 2465.
- [96] Z. Herman, J. Žabka, Z. Dolejšek, M. Fárník, *Int. J. Mass Spectrom.* 192 (1999) 191.
- [97] L. Mrázek, J. Žabka, Z. Dolejšek, J. Hrušák, Z. Herman, *J. Phys. Chem.* 104 (2000) 7294.
- [98] M.A. Parkes, J.F. Lockyear, S.D. Price, *Int. J. Mass Spectrom.* 280 (2009) 85 and references cited therein.
- [99] J.D. Fletscher, M.A. Parkes, S.D. Price, *Chem. Eur. J.* 19 (2013) 10965.
- [100] P. Tosi, R. Correale, W. Lu, S. Falcinelli, D. Bassi, *Phys. Rev. Lett.* 82 (1999) 450.
- [101] J. Roithová, D. Schröder, *J. Am. Chem. Soc.* 128 (2006) 4208.
- [102] J. Roithová, C.L. Ricketts, D. Schröder, *Int. J. Mass Spectrom.* 280 (2009) 32.
- [103] J.A. Laramee, J.J. Carmody, R.G. Cooks, *Int. J. Mass Spectrom.* 31 (1979) 333.
- [104] A.K. Shukla, J.H. Futrell, *J. Mass Spec.* 35 (2000) 1069.
- [105] Z. Herman, J.H. Futrell, B. Friedrich, *Int. J. Mass Spectrom.* 58 (1984) 181.
- [106] J. Biggerstaff, K. Qian, S. Howard, A.K. Shukla, J.H. Futrell, *Chem. Phys. Lett.* 151 (1988) 5071.
- [107] K. Qian, A.K. Shukla, J.H. Futrell, *J. Chem. Phys.* 92 (1990) 5988.
- [108] A.K. Shukla, J.H. Futrell, *Mass Spec. Rev.* 12 (1993) 211.
- [109] V. Grill, J. Shen, C. Evans, R.G. Cooks, *Rev. Sci. Instrum.* 72 (2001) 3149 and references cited therein.
- [110] G. Tsapralis, H. Nair, A. Somogyi, V.H. Wysocki, W. Zhong, J.H. Futrell, S.G. Summerfield, S.J. Gaskell, *J. Am. Chem. Soc.* 121 (1999) 5142.
- [111] A.R. Dongre, A. Somogyi, V.H. Wysocki, *J. Mass Spectrom.* 31 (1996) 339.
- [112] J. Laskin, J.H. Futrell, *J. Am. Soc. Mass Spectrom.* 14 (2003) 1340.
- [113] V.H. Wysocki, K.E. Joyce, C.M. Jones, R.L. Beardsley, *J. Am. Soc. Mass Spectrom.* 19 (2008) 190.
- [114] J.H. Futrell, J. Laskin, *Encyclopedia of Spectroscopy and Spectrometry*, Academic Press, 2010, pp. 2778–2787.
- [115] A.K. Shukla, J.H. Futrell, *Int. J. Mass Spectrom.* 223–224 (2003) 783.
- [116] Z. Herman, *J. Am. Soc. Mass Spectrom.* 14 (2003) 1360.
- [117] Z. Herman, J. Žabka, A. Pysanenkov, *J. Phys. Chem. A* 113 (2009) 14838.
- [118] J. Žabka, Z. Dolejšek, Z. Herman, *J. Phys. Chem. A* 106 (2002) 10861.
- [119] J.A. Burroughs, S.B. Wainhaus, L. Hanley, *J. Phys. Chem.* 98 (1994) 109.
- [120] J. Kubišta, Z. Dolejšek, Z. Herman, *Eur. Mass Spectrom.* 4 (1998) 311.
- [121] H.L. de Clercq, A.D. Sen, A.K. Shukla, J.H. Futrell, *Int. J. Mass Spectrom.* 212 (2001) 491.
- [122] K. Park, K. Song, W.L. Hase, *Int. J. Mass Spectrom.* 265 (2007) 326/.
- [123] L. Yang, O.A. Mazyar, U. Lourderaj, J. Wang, M.T. Rodgers, E. Martinez-Nunez, S.V. Addepalli, W.L. Hase, *J. Phys. Chem. C* 112 (2008) 9377.